Indian Journal of Science and Technology, Vol 8(18), DOI: 10.17485/ijst/2015/v8i18/53103, August 2015
ISSN (Print) : 0974-6846
ISSN (Online) : 0974-5645

Performance Analysis of DTC-CSI fed IPMSM Drive at Very Low Speed with Stator Resistance Compensation

N. Panneer Selvam[1]*, V. Rajasekaran[2] and N. Jayanthi[1]

[1]V.S.B Engineering College, Department of Electrical and Electronics Engineering, Karur–639111, Tamil Nadu, India; panneerselvamno1@gmail.com

[2]PSNA College of Engineering and Technology, Department of Electrical and Electronics Engineering, Dindigul-624622,Tamil Nadu, India

Abstract

Objectives: This paper proposed to enhance the performance of Direct Torque Control (DTC) of CSI fed IPMSM drive with online stator resistances estimation of using PI controller. **Methods/Analysis**: Direct Torque Control (DTC) CSI fed IPMSM drives have widely used because of its high dynamic performance and no position sensor requires. This scheme is need less parameter to estimate of motor torque and stator flux linkages by using the stator quantities such as voltage and current. The estimation is dependent only the machine parameter such as stator resistance. **Findings**: At low speed operation the stator resistance is varying due to temperature and frequency which degrade the system performance by introducing errors in flux linkage and motor torque during estimation. Hence the stator resistance compensation is essential at low speed. The error between estimated stator flux and its reference value are used to estimate the stator resistance by using PI controller. For the first time, it is demonstrated in this paper for DTC with CSI fed IPMSM drive system. **Conclusion/Application**: It is demonstrated for the first time for DTC with CSI fed IPMSM drives. The performance of the stator resistance estimators and torque and flux responses of the drive are investigated with the help of MATLAB/SIMULINK software and hardware. The results show that the proposed methods ensure the reliable and high-performance operation of the drive.

Keywords: Current Source Inverter, Direct Torque Control, IPM Synchronous Motor, PI Controller, Stator Resistance Compensation

1. Introduction

In present day IPMSM drive widely used in industry compared with other drives due to its advantages such as simple rotor construction, better efficincy, less maintenance high power density and improved power factor. Comparing with Induction Machine (IM), IPMSM has generate constant rotor flux. It is worth mentioning that with the development of new permanent magnet materials, the power range of the IPM synchronous machine has extended upto 30 M wand its make a good option for high-power medium-voltage drive applications.

Due to inherent disadvantages in voltage source inverter[1], a Current Source Inverter (CSI) Figure 1 has been preferred for a wide range speed control[2,3]. The control techniques[4-6] are used to improve the performance of IPMSM and reduced the harmonics. The current source inverter fed drive finds high power application and where fast dynamic response is not needed. No need of additional circuit for four quadrant operation in CSI fed drives unlike VSI fed drives[7]. In CSI drives the dc link reactor limits the rate of rise of current under short circuit conditions, so the drives can be easily protected under short circuit and thus results in improved reliability of the drive[8,9]. Medium-voltage level configuration of the current-source drive system shown in Figure1, which consists of a Pulse Width Modulation (PWM) Current-Source Rectifier (CSR), a DTC-CSI, input and out put filters, a dc-link inductor.

*Author for correspondence

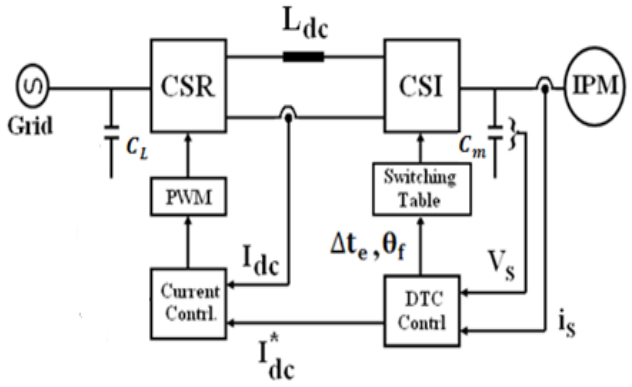

Figure 1. Basic structure of DTC-CSI fed drive.

A conventional scheme of DTC fed IPMSM control as shown in Figure 2. The stator flux links are obtained by integrating the back EMF of the stator winding and forming a vector that is rotating around the rotor of the machine, that it can be modified in magnitude and phase depending on the applied current vector.

The idea of combining the advantages of DTC in PMSM were presented in the '90 as reported in[10-14] and from then many authors have proposed drive applications to improve this technique. DTC produces torque response as fast as possible, due to its simplicity. Estimation of stator flux by means of stator resistance is the main limitation of this method. The stator resistance variation due to the temperature gets changes such changes degrade the drive performance by means of errors in the estimated magnitude and position of the flux linkage vector. This affects the determination of the electromagnetic torque, especially at low speeds. At low speeds the stator resistance voltage drop is relatively large and may become comparable to the back emf. If the stator resistance deviates from the one used in the controller, the drive may become unstable at low speed. To overcome the problem of stator resistance variation several control schemes have been proposed which has some demerits such as restriction to speed control range of the drives and problem ofconvergence[15-18]. In this paper, the effect of stator resistance variation is discussed for CSI-FED IPMSM and the stator resistance is estimated by using a PI estimator. A signal proportional to stator resistance change is developed using the error between the reference and actual stator flux linkage. The controller performance is examined by both extensive simulation and experimental studies.

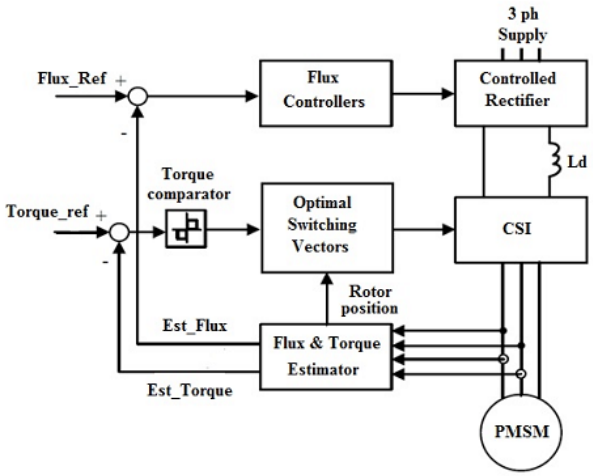

Figure 2. Conventional DTC-CSI fed PMSM drive.

2. Mathematical Model of PMSM

Stator magnetic flux vector λ_S and rotor magnetic flux vector λ_M, can be denoted on the rotor flux (dq), stator flux (xy) reference system as shown in Figure 3.The angle between the stator and rotor magnetic fluxes are denoted by the load angle (δ). δ is also constant for constant torque. In this case the speed of stator and rotor is constant. However δ varies for different loads. In order to control the increase of the torque, either the stator current rotation speed or the variation of δ is controlled.

The machine equation of IPM motor are the follows:

$$\lambda_{ds} = L_{ds} i_{ds} + \lambda_M \tag{1}$$

$$\lambda_{qs} = L_{qs} i_{qs} \tag{2}$$

$$v_{ds} = R_s i_{ds} + \frac{d}{dt}\lambda_{ds} - \omega_r \lambda_{qs} \tag{3}$$

$$v_{qs} = R_s i_{qs} + \frac{d}{dt}\lambda_{qs} - \omega_r \lambda_{ds} \tag{4}$$

$$T_e = \frac{3}{2} P\left[\lambda_M i_{qs} - \left(L_{qs} - L_{ds}\right) i_{ds} i_{qs}\right] \tag{5}$$

is obtained[7]. The symbols of parameters are as follows;

λ_{ds} d axis stator magnetic flux,
λ_{qs} q axis stator magnetic flux,
λ_M rotor magnetic flux,
L_{ds} d axis stator leakage inductance,
L_{qs} q axis stator leakage inductance,

R_s stator winding resistance,
T_e electromagnetic torque,
p Number of pole pairs

Using the transformation in Equation 6 and Figure 3, the expressions (7) are obtained, using 7, Equation5, can be transformed into Equation 8

$$\begin{bmatrix} F_d \\ F_q \end{bmatrix} = \begin{bmatrix} \cos\delta & -\sin\delta \\ \sin\delta & \cos\delta \end{bmatrix} \begin{bmatrix} F_x \\ F_y \end{bmatrix} \tag{6}$$

Here the voltage, current and magnetic flux are represented by F.
Using Figure 3.

$$\sin\delta = \frac{\lambda_{qs}}{|\lambda_s|}$$

$$\cos\delta = \frac{\lambda_{ds}}{|\lambda_s|} \tag{7}$$

is obtained. The expression $|\lambda_s|$ represents the amplitude stator magnetic flux. When the necessary terms are replaced using Figure 3, the following equations are obtained.

$$T_e = \frac{3}{2} p\left[\lambda_{ds}\left(i_{sx}\sin\delta + i_{sy}\cos\delta\right) - \lambda_{qs}\left(i_{sx}\cos\delta - i_{sy}\sin\delta\right)\right]$$
$$= \frac{3}{2} p\left[i_{sx}\frac{\lambda_{ds}\lambda_{qs}}{|\lambda_s|} + i_{sy}\frac{\lambda^2_{ds}}{|\lambda_s|} - i_{sx}\frac{\lambda_{ds}\lambda_{qs}}{|\lambda_s|} + i_{sy}\frac{\lambda^2_{qs}}{|\lambda_s|}\right]$$

$$T_e = \frac{3}{2} p|\lambda_s| i_{sy} \tag{8}$$

It is clear that the electromagnetic torque and the y-axis component of the stator current are directly proportional to each other[11]. Direct Control of the stator current provides proper selection of the current switching vectors. Less parameter dependent is the main advantage of stator current control. In practical applications, the estimation technique shown in Equation 5 requires saturation-dependent inductances. Therefore in Equation 8 direct torque control over the stator current control is more convenient.

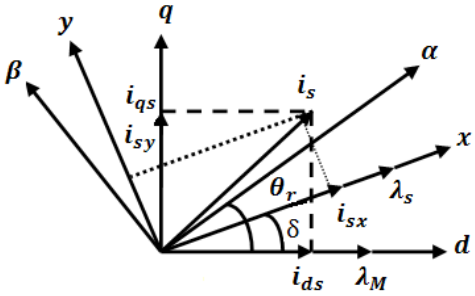

Figure 3. Stator and rotor magnetic fluxes in different reference systems.

3. Drive System and Control Scheme

The block diagram of the proposed current source drive system fed IPM and its direct torque control scheme is illustrated in Figure 4. The drive system consists of a PWM CSR and a DTC-CSI. In this control scheme the stator quantities are used to estimate the stator flux, torque, stator resistance.

3.1 DTC Scheme for PMSM

Selection of stator current vectors according to the differences between the reference and actual torque and flux linkage is the basic principle. In this drive we use DTC system because of high dynamic performance and less parameter usage except the stator resistance. Figure 4 shows the block diagram of the DTC for Permanent Magnet Synchronous Motor (PMSM) drive with a stator resistance estimator. In DTC, the stator flux, torque are estimated by using the estimated stator resistance and Equation 3 and 4 becomes,

$$v_{ds} = \check{R}_s i_{ds} + \frac{d}{dt}\lambda_{ds} - \omega_r \lambda_{qs} \tag{9}$$

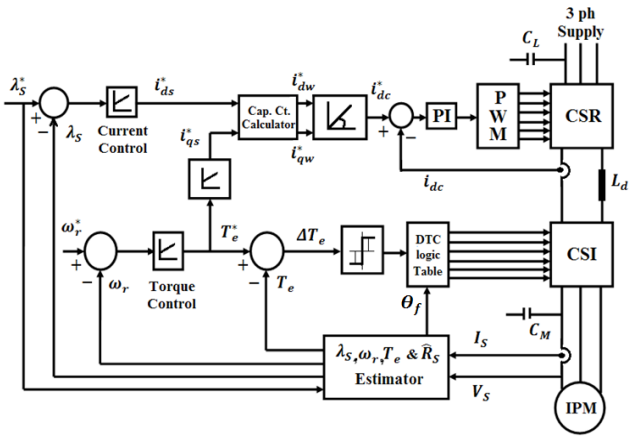

Figure 4. Proposed diagram for DTC fed PMSM drive system.

$$v_{qs} = \breve{R}_s i_{qs} + \frac{d}{dt}\lambda_{qs} - \omega_r \lambda_{ds} \tag{10}$$

The magnitude of flux linkage is given by

$$|\lambda s| = \sqrt{\left(\lambda^2_{ds} + \lambda^2_{qs}\right)} \tag{11}$$

$$\angle\theta_s = \tan^{-1}\frac{\lambda_{qs}}{\lambda_{ds}} \tag{12}$$

and the electromagnetic torque also obtained by the following equation,

$$T_e = \frac{3}{2} p |\lambda_s| i_{sq} \tag{13}$$

Where

$\hat{R}_S$ - estimated stator resistance.

p - number of pole pairs

The stator flux linkage space vector in the stator reference frame can be obtained from

$$\bar{\lambda}_s = \left(\lambda_{ds} + j\lambda_{qs}\right)e^{j\theta_s} \tag{14}$$

Finally the sub transient flux linkage space vector can be obtained from

$$\bar{\lambda}^{"}_S = \bar{\lambda}_s - L^{"}_s \bar{i}_s \tag{15}$$

However to improve the performance of IPMSM at low frequencies the $\bar{\lambda}^{"}_S$ is added with $T\left(\bar{u}_s - R_s \bar{i}_s\right)$, where T is appropriately chosen, and then the resulting component is multiplied by $1/(1 + pT)$ where p is derivative. It results in,

$$\hat{\bar{\lambda}}^{"}_S = \frac{\bar{\lambda}^{"}_s + T\left(\bar{v}_s - R_s \bar{i}_s\right)}{\left(1 + pT\right)} \tag{16}$$

It should note that the rate of change of the stator flux linkage space vector is equal to $\bar{v}_s - R_s \bar{i}_s$ is estimated from the measured stator voltage and currents. Thus it is obtained by using the stator voltage equation which gives accurate estimation at higher stator frequencies. It follows that the stator subtransient flux linkage space vector can be more accurately estimated by using the following

$$\hat{\bar{\lambda}}^{"}_S = \bar{\lambda}^{"}_s - L^{"}_s \bar{i}_s \tag{17}$$

and then the flux amplitude calculated and find the sector with 60 degrees in α - β plane as shown in Figure 5.

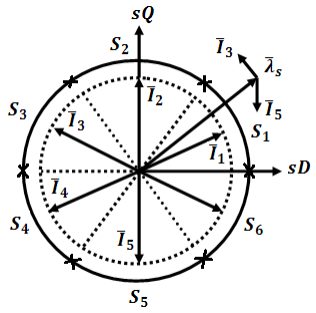

Figure 5. α - β plane.

Flux error is used to produce a constant current and estimate the stator resistance and not introduced to the switching table in a CSI fed PMSM drive in this topology[19], the torque error is the only input in the basic DTC scheme. The optimal current switching vector look-up table is presented in Table 1. Which used in the standard DTC strategy shown in Figure 2. Stator flux vector resides in α - β plane and its sector denotes *Sx* (x = 1,…,6) as shown in Figure 5. The torque error Δ*Te* is obtained at the output of a three-level hysteresis controller, the non-sinusoidal supply that is inhered in CSI operation produces larger torque ripples especially at low speed, which can be easily reduced by proposed technique.

3.2 Effect of Filter Capacitor on System Control

The filter capacitors is connected at the output of the CSI inverter. This means that a portion of the inverter currents go through the capacitors. In this section the effect of the filter capacitors on the system control is investigated.

The inverter reference currents can be expressed as follows:

$$i^*_{dw} = i_{cd} + i^*_{ds} \tag{18}$$

$$i^*_{qw} = i_{cq} + i^*_{qs} \tag{19}$$

Where i_{cd} and i_{cq} are the estimated capacitor *d*–*q* axis currents.

Table 1. Current Switching Vector of DTC-CSI

ΔT_e	S_1	S_2	S_3	S_4	S_5	S_6
1	I_3	I_4	I_5	I_6	I_1	I_2
0	*0*	*0*	*0*	*0*	*0*	*0*
–1	I_6	I_1	I_2	I_3	I_4	I_4

$$i_{cd} = -\omega_r v_{qs} C_m \quad (20)$$

$$i_{cq} = \omega_r v_{ds} C_m \quad (21)$$

Where C_m, ω_r, *vds* and *vqs* are the inverter-side filter capacitance, motor angular frequency, and stator *d*-axis and *q*-axis voltages, respectively. The estimated capacitor currents are usually simplified and which is used to reduce the sensitivity and noise.

4. Stator Resistance Variation Effect

In DTC control to estimate stator flux linkage is dependent proportional to the stator resistance 'Rs'. During high speed 'Rs' does not effect and it can be neglected. Stator resistance 'Rs' is very significant at low speed because variation of temperature and frequency. Due to change of stator resistance the parameter stator flux and electric torque mismatch between the set value and estimated value results the drive system become unstable. Therefore the overall performance of the DTC system is degrading. To overcome this stator resistance compensation is essential.

4.1 PI Stator Resistance Estimators

The block diagram of PI control stator resistance compensator as shown in Figure 6.The principle of this technique is due to change of stator resistance cause a change in stator current and stator flux linkage $\boldsymbol{\lambda}_S$. The error between the estimated value of $\boldsymbol{\lambda}_S$ and its reference λ^*_S is proportional to the stator resistance change. The Equations for PI resistance estimator are given by

$$\hat{R}_S = \Delta R_S + R_{SO}$$

$$\Delta R_S = \left(k_p + k_i \frac{1}{s} \right) \Delta \lambda_S$$

Where K_p and K_I are the proportional gain and integral gain of the PI estimator.

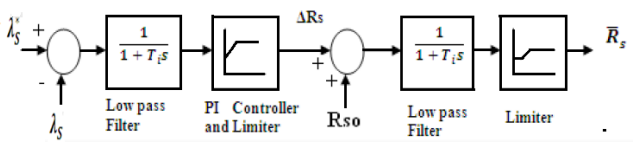

Figure 6. Block Diagram of PI Stator resistance compensation.

The incremental value of stator resistance ΔR_S is obtained when the error between the stator fluxes goes through a low passes filter, PI controller and limiter. Low pass filter has very low cutoff frequency in order to eliminate high frequency components contained in the estimated stator flux. Select the filter time constant T_1 is smaller than that of the adaptation time constant, the low pass filter does not generate any adverse effect on the stator resistance adaptation. Previously estimated stator resistance value of R_{SO} is continuously added with incremental value of stator resistance ΔR_S. Finally the estimated stator resistance value is $\hat{R}_s$ obtained as the output of another low pass filter and limiter. It is necessary for a smooth variation of the estimated stator resistance value. This final signal $\hat{R}_s$ is the updated stator resistance and it can be used directly in the controller.

5. Results and Discussion

5.1 Simulation Results

The simulation results of the proposed PI resistance estimator with direct torque control strategy has been verified by using MATLAB/SIMLINK. Appendix shows that the parameters were performed on a 3.5Kw, 4 pole IPMSM motor. Figures 7(a) and 7(b) shows that the simulation results for DTC drive CSI fed IPMSM operated with 200 r/min and standstill without compensation of Rs respectively and torque has more ripples when the Rs is uncompensated. So mismatch between the estimated stator resistance and its set value can make the drive controller is unstable. The proposed stator resistance compensation is to overcome this instability. Extensive simulation has been performed to investigate the effect of stator resistance variation. The performance of the controller Figure 8(a) depicts the estimator performance due to 25 percent increase in R_S when the machine is running at -200r/min to 200r/min. In addition, Figure 8(b) shows the performance of the speed (0-200 r/min) and torque with 25percent increased value of R_S. Figure 8(c) shows the estimation algorithm due to 25percent increase in R_S when the machine at standstill. Load applied to the motor shaft is half of the rated value at all speed. The results prove that the proposed stator resistance estimator is very effective for both low and high speeds as it is able to identify the actual stator resistance value within a short time frame. Nevertheless, the sensitivity of the estimator is low when the load is small.

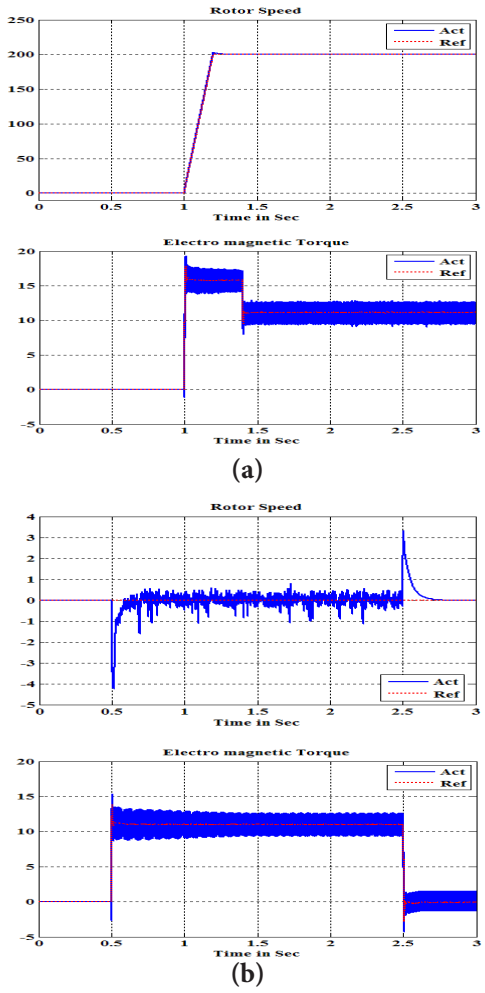

Figure 7. Without compensation of RS. **(a)** Simulation results for rotor speed and torque (0-200rpm) (Without RS Compensation) **(b)** Simulation results for rotor speed and torque at stand still (without RS compensation)

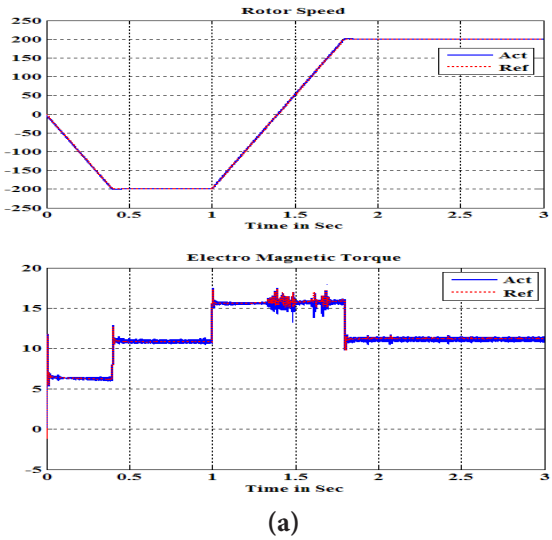

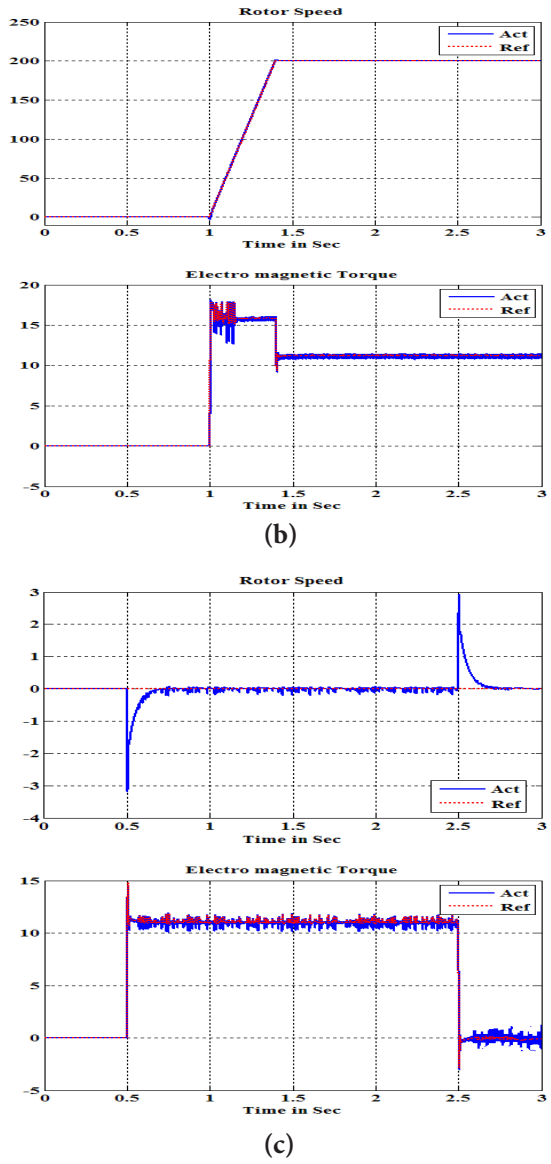

Figure 8. Simulation results with RS compensation. **(a)** Sensorless full load speed reversal from -200 to +200 rpm **(b)** Startup response with full load **(c)** Sensorless full load dynamics at stand still

5.2 Experimental Results

The performance of the proposed sensorless drive scheme was tested experimentally. The experimental block diagram of the sensorless drive is shown in Figure 9. The mechanical part of the drive contains the IPMSM and a loading DC motor. A Free scale DSP 56F8037 digital signal processor is used to carry out the real-time algorithm. In an inverter a three-phase IGBT intelligent power module is used, C language was used for coding of real-time

control software. All measured and controller internal variables are accessible through the serial link to the PC, where graphical data-analysis software can be run. The sampling time of the measurements and computation of control algorithm is 200 μs. The controllers of quantities in the control structure of the AC drive were adjusted accordance with the parameters are used in IPMSM is shown in Appendix.

The speed reversal from -200 to +200 with half load is shown in Figure 10(a). The reference speed, actual speed, reference torque and actual torque are shown. The actual speed follows the reference speed during the transient interval. The dynamic response during acceleration from zero to 200 r/min is shown in Figure 10(b). The machine was originally operated at zero speed (shown Figure 10(c) with step load changes, which occur very fast and zero speed is holding satisfactorily. The estimated speed tracks the actual speed closely during the transient and steady state and also show that ripples of torque is minimized. Figure 10 shows that effectiveness of the stator resistance estimator. Figures 11(a) and (b) shows that the responses of the resistance estimator with 25 percent and 50percent increased value of the stator resistance *Rs* respectively. In both cases, the machine is operated with half full load and it can be observed that the resistance estimator is performed well during the low and high speed operation.

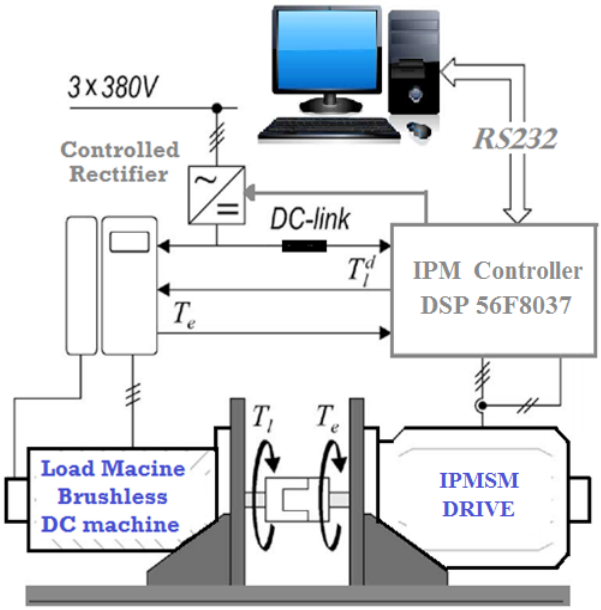

Figure 9. Block diagram for experimental set up.

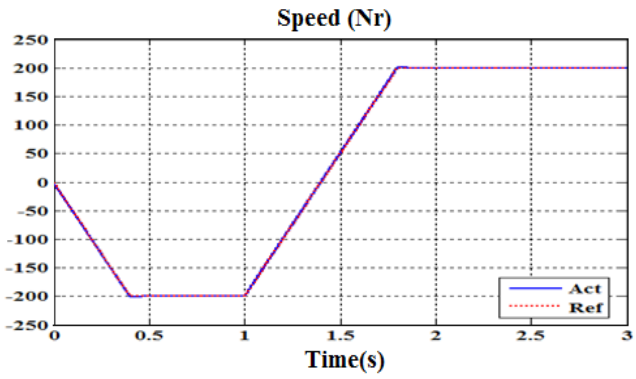

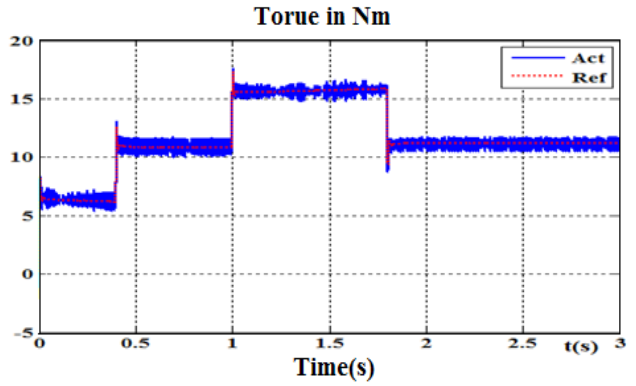

(a)

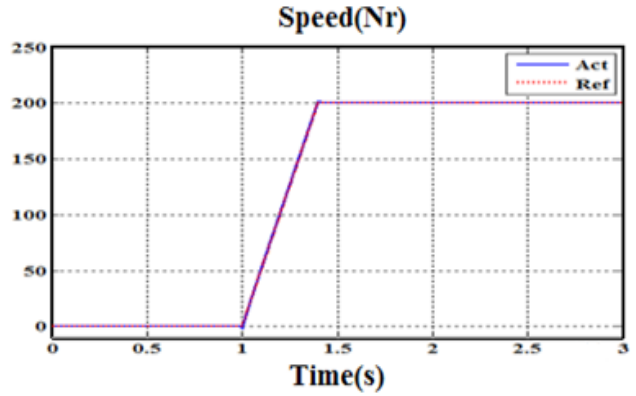

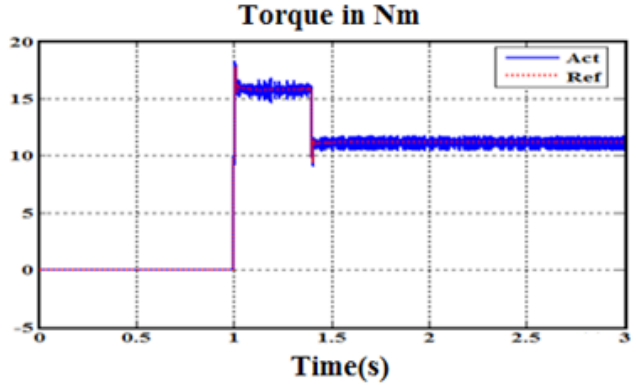

(b)

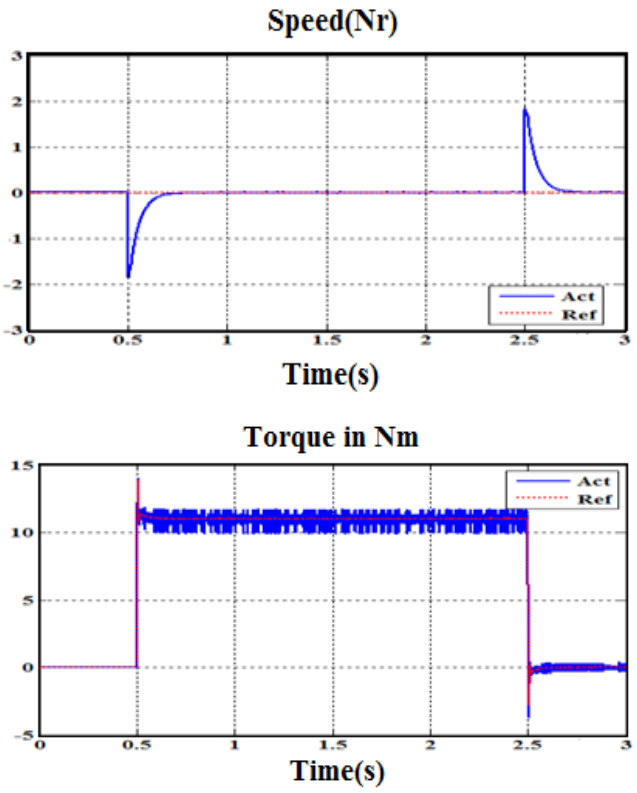

(c)

Figure 10. Experimental results. **(a)** Speed reversal from –200 to + 200 rpm **(b)** Start up response with full load **(c)** Sensorless full load dynamics at stand still

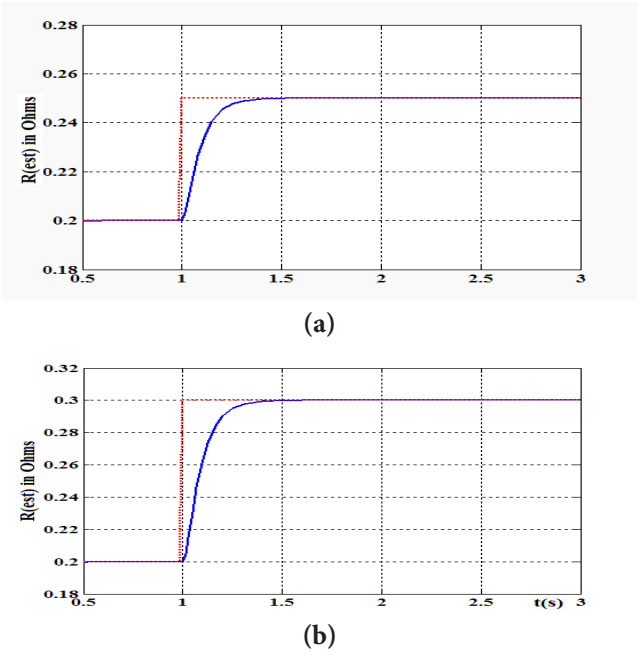

(a)

(b)

Figure 11. Estimated stator resistance **(a)** increased 25% **(b)** increased 50%.

6. Conclusion

DTC drive system become unstable if the estimated resistance value differs from that of actual stator resistance value. The error between stator flux λ_s and its reference λ_s^* is used to estimate the stator resistance. The stator flux linkage λ_s is estimated from measured stator current and voltage. The error between actual and estimated flux linkage is processed through a PI controller. The design of a PI controlled stator resistance estimator is easier compared to other controller and it is implemented in DTC-CSI fed IPMSM drives very first time. The proposed control system was to deliver high performance at low speed oprations. Software and hardware results at low speeds including zero speed and 200 r/min are demonstrated and prove that the system performed well at low speed.

7. References

1. Lipo TA. Recent progress in the development of solid state ac motor drives. IEEE Trans Power Electronics. 1988 Apr; 3(2):105–17.
2. Beerten J, Verveckken J, Driesen J. Predictive direct torque control for flux and torque ripple reduction. IEEE Transactions on Industrial Electronics. 2010 Jan; 57(1):404–12.
3. Wu B, Dewan SB, Slemon GR.PWM CSI inverter for induction motor drives. IEEE Transactions on Industry Applications.1992 Jan/Feb; 28(1):64–71.
4. Pal S, Dalapati S. Digital simulation of two level inverter based on space vector pulse width modulation. Indian Journal of Science and Technology. 2012 Apr; 5(4).
5. Asadi M, Farahani HF. Evaluation effective parameters on the output current harmonics of SHE-PWM voltage source inverters. Indian Journal of Science and Technology.2012, Mar; 5(3).
6. Pandian G, Rama Reddy S. Simulation and analysis of multilevel inverter fed induction motor drive. Indian Journal of Science and Technology. 2009 Feb; 2(2).
7. Bose BK. Adjustable speed ac drives: a technology status review. IEEEProceedings.1982 Feb; 70(2):116–35.
8. Chattpadhyay AK. Current source inverter fed induction motor drives a state of the art research review. JIE. 1991; 37(1):34–46.
9. Banerjee D, Ranganathan VT. Load-Commutated SCR current-source-inverter-fed induction motor drive with sinusoidal motor voltage and current. IEEE Transactions on Power Electronics. 2009 Apr; 24(4):1048–61.

10. Tang P, Yang G, Luo M, Li T. A current control scheme with tracking mode for PMSM system.1st International Symposium on Systems and Control in Aerospace and Astronautics; 2006. p. 872–6.
11. Park Y, Sul S-K, Ji J-K,Park Y-J. Analysis of estimation errors in rotor position for a sensorless control system using a PMSM. Journal of Power Electronics. 2012 Sep; 12(5):748–57.
12. Zhong L, Rahman MF, Hu WY, Lim KW. Analysis of direct torque control in permanent magnet synchronous motor drives. IEEE Tran on Power Electronics. 1997 May; 12(3).
13. Rahman MF, Zhong L, Lim KW. A direct torque controlled interior permanent magnet synchronous motor drive incorporating field weakening. IEEE Tran Industry applications. 1988 Nov/Dec; 34(6):1246–53.
14. Singh V, Gupta M. Direct Torque Control (DTC) of PMSM using space vector modulated inverter- A Simulink, approach. International Journal of Engineering and Innovative Technology. 2012 Mar; 1(3).
15. Habetler TG, Profumo F, Griva G, Pastorelli M, Bettini A. Stator resistance tuning in a stator flux field oriented drive using an instantaneous hybrid flux field oriented drive using an instanteneous hybrid flux estimator. Conference Record EPE Conference;1993; Brighton, UK. p. 292–9.
16. Kwon C-K. An on-line rotor resistance estimator for induction machine drives. Journal of Power Electronics. 2009 May; 9(3):353–63.
17. Kerkman RJ, Seibal BJ, Rowan TM, Schlegel D.A new flux and stator resistance identifier for AC drive systems. Conference Record, IEEE-IAS; 1995 Oct; Orlando, Florida. p. 310–8.
18. Malik SM, Elbuluk E, Zinger DS.PI and fuzzy estimators for tuning the stator resistance in direct torque control of induction machines. IEEE Tran on Power Electronics. 1998 Mar; 13(2):279–87.
19. Vas P. Sensorless Vector and Direct Torque Control. Oxford University Press; 1998.

Appendix

Number of pole pairs **Stator Resistance(R_S)**	**4** **0.22Ω**
Magnetic Flux	0.175 Wb
Voltage	380 v
Base speed	1500rpm
Electromagnetic Torque	22 Nm
Inductance (L_d)	8.5e-03
Inductance (L_q)	8.5e-03